Am J Transl Res 2021;13(4):2094-2110
www.ajtr.org /ISSN:1943-8141/AJTR0120310

Original Article

Network pharmacology-guided mechanism study uncovers inhibitory effect of Mahuang Decoction on lung cancer growth by impeding Akt/ERK signaling pathways

Ya Pan[1,2,3,4*], Yuhong Chen[2,3,4,5*], Chunnuan Wu[2,3,4,6], Jun Ai[7], Yun Wang[2,3,4,8], Junrong Jia[2,3,4,9], Liren Liu[1,2,3,4]

[1]Department of Gastrointestinal Cancer Biology, Tianjin Medical University Cancer Institute & Hospital, Tianjin 300060, China; [2]National Clinical Research Center for Cancer, Tianjin 300060, China; [3]Key Laboratory of Cancer Prevention and Therapy, Tianjin 300060, China; [4]Tianjin's Clinical Research Center for Cancer, Tianjin 300060, China; [5]The First Surgical Department of Breast Cancer, Tianjin Medical University Cancer Institute & Hospital, Tianjin 300060, China; [6]Department of Pharmacy, Tianjin Medical University Cancer Institute & Hospital, Tianjin 300060, China; [7]The State Key Laboratory of Medicinal Chemical Biology (SKLMCB), Nankai University, Tianjin 300071, China; [8]Department of Integrated Traditional & Western Medicine, Tianjin Medical University Cancer Institute & Hospital, Tianjin 300060, China; [9]Public Laboratory, Tianjin Medical University Cancer Institute & Hospital, Tianjin 300060, China. [*]Equal contributors.

Received August 14, 2020; Accepted December 1, 2020; Epub April 15, 2021; Published April 30, 2021

Abstract: Lung cancer (LC) ranks the leading cause of cancer-related death worldwide, due partially to the unsatisfactory therapeutic effect of the mainstream treatment. Alternatively, Chinese herb medicine (CHM) offers a bright perspective for treating complex diseases. Mahuang Decoction (MHD), a classic CHM formula, has been widely used in treating respiratory diseases in China for centuries, but its action mechanism has yet to be fully investigated. In this study, we first systemically explore the action mechanism of MHD by using network pharmacology and bioinformatic analysis tools, which uncovered a potential "new use of old drug" for MHD in cancer treatment. The therapeutic effect of MHD on LC was then validated by oral administration of MHD in the immunodeficient mice bearing xenografted LC tumors. To better understand the pharmacological activity of MHD against LC, we next constructed a drug/disease-target PPI network composed of 252 putative core therapeutic targets of MHD using Cytoscape. The subsequent enrichment analysis for these targets suggested that MHD could affect the apoptosis and cell cycle of LC cells via impeding Akt/ERK signaling pathways. Notably, these *in silico* analysis results were further validated by a series of cellular functional and molecular biological assays. Thus, our results show that MHD holds a great potential in LC treatment.

Keywords: Mahuang Decoction (MHD), lung cancer (LC), Chinese herb medicine (CHM), network pharmacology, bioinformatics, Akt/ERK signaling pathways

Introduction

Lung cancer (LC) is the leading cause of cancer-related death worldwide. More than half of the LC patients are diagnosed at advanced stages, and thus miss the opportunity for curative surgery [1, 2]. Currently, radiotherapy, chemotherapy and targeted therapy are mainstream treatments for advanced LC [3]. However, the overall therapeutic effect of these treatments is unsatisfactory [4], therefore novel approaches are needed to improve outcomes for LC patients. Chinese herb medicine (CHM), as an essential component of Traditional Chinese medicine (TCM), has been widely used to treat various diseases in China for thousands of years. Recent studies showed that CHM offers an attractive treatment option for treating complex diseases such as cancer, owing to its unique clinical effects [5-8].

Mahuang Decoction (MHD) is a classic CHM formula from Treatise on Febrile Diseases. With its distinct expectorant and cough relieving eff-

ects, MHD has been documented to treat various respiratory diseases since the 2nd century AD. It is composed of four herbs, including *Ephedrae Herba* (Ma-Huang, MH), *Cinnamomi Ramulus* (Gui-Zhi, GZ), *Armeniacae Semen Amarum* (Xing-Ren, XR), and *Glycyrrhizae Radix Et Rhizoma* (Gan-Cao, GC) (**Figure 1A**). Recent studies have demonstrated that MHD has desirable pharmacological activities in treating asthma through mitigating airway inflammation and febrile [9, 10]. More recently, MHD was reported to have adjuvant therapeutic effects on chronic cough and malignant pleural effusion [11, 12]. However, the action mechanism of MHD as well as its potential clinical application beyond respiratory diseases has yet to be fully evaluated.

In the present study, we first conducted a virtual study to explore the action mechanism of MHD using network pharmacology and bioinformatic analysis tools, which suggested a "new use of old drug" for MHD in cancer treatment. Due to the well-established therapeutic effect of MHD on respiratory diseases, we next determined the growth of LC cells on immunodeficient mice after orally administered with MHD. Having validated the therapeutic effect of MHD on LC cells *in vivo*, we next performed a series of *in vitro* assays guided by network pharmacology and bioinformatics, so as to provide some insights into the action mechanism of MHD against LC.

Material and methods

Cell culture and reagents

Human LC LTEP-A-2 and Glc-82 cell lines were obtained from the China Infrastructure of Cell Line Resources (School of Basic Medicine Peking Union Medical College, China) and were maintained in RPMI-1640 supplemented with 10% (v/v) FBS and 100 U/ml streptomycin/penicillin in 5% CO_2 at 37°C. Antibodies against Bcl-2, Bax, Caspase 9/p35/p10, Cyclin D1 and beta-actin were bought from Proteintech. Antibodies against Cyclin B1, Cyclin A2, p-Akt (S473), pan-Akt, p-ERK (T202/Y204) and pan-ERK were bought from CST. Antibody against CDK2 was obtained from Abcam. The MHD was provided by the Tianjin Medical University Cancer Institute & Hospital TCM Pharmacy. The quality matching (g) of the four ingredients from MHD was as follows: MH:GZ:XR:GC = 3:2:2:1. The final concentration of MHD was 30 mg/ml.

Candidate ingredients composition of MHD

The chemical composition of all the 4 herbs was mainly obtained from Traditional Chinese Medicine Systems Pharmacology (TCMSP) Database (http://lsp.nwu.edu.cn/tcmsp.php) and Traditional Chinese Medicine Integrated Database (TCMID) (http://www/megabionet.org/tcmid/) in 2018, and in TCMSP, the parameters for selection of active ingredients were set as oral bioavailability (OB) ≥ 30% and drug-likeness (DL) ≥ 0.18 as standard [13, 14]. In addition, literature-mining method (www.CNKI.net) was used to search for the ingredients that failed to meet the above parameters but have been reported to contain in the herbs.

Identifying putative drug targets and known LC-related targets

The systematic drug targeting approach was utilized to identify potential targets for medicinal composition of MHD [15]. The potential drug targets were obtained from TCMSP and SwissTargetPrediction databases (http://www.swisstargetprediction.ch/) (Supplementary Table 1). The known LC-related targets were obtained from Gene Expression Omnibus (GEO) database (Supplementary Table 2). Four gene expression datasets (GSE22863, GSE27262, GSE43458 and GSE101929) derived from human LC and adjacent normal tissues were included. The protein-protein interaction (PPI) data were analyzed using Bisogenet, a key plugin of Cytoscape, and the final result was integrated into a single graph from six analyses of the obtained PPI datasets.

Systematic network construction and correlation enrichment analysis

The interaction networks for the putative drug targets of MHD and the known LC-related targets based on the data obtained from the Bisogenet plugin were constructed and visualized using Cytoscape (Version 3.2.1) [16]. After merging the above two PPI networks, the topology parameters of each node in the merged network was calculated using CytoNCA, another important plugin in Cytoscape. The node with a score twice higher than the median of "Degree centrality" (DC) was consid-

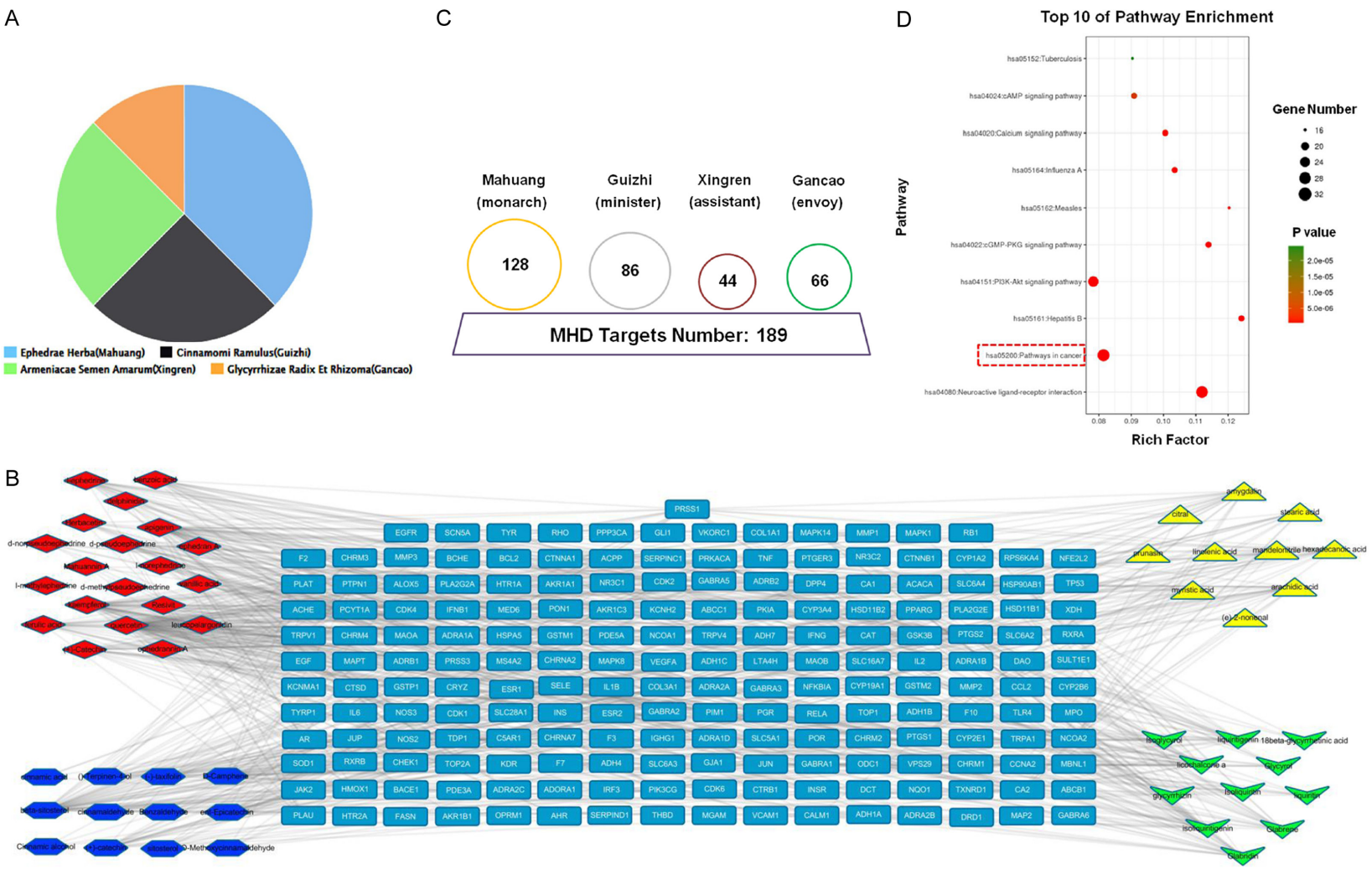

Figure 1. Construction of the MHD ingredient-target systematic network and enrichment analysis of the putative targets. A. The quality matching diagram of four important pharmaceutical ingredients from MHD (MH, GZ, XR, GC). B. The systematic network was constructed by linking the candidate active ingredients and their putative targets of the 4 herbs contained in MHD. C. The diagram of candidate drug target number of different 4 herbs in MHD formulated in accordance with the TCM principle of monarch, minister, assistant and envoy. D. Putative drug targets were enriched in the representative signalling pathways using DAVID v6.8 ($P < 0.05$).

ered important and appeared in the new systematic network (See more details in Supplementary Table 3). Functional and pathway enrichment analyses of the obtained putative and core targets were performed as before [17-19].

Xenografted immunodeficient mouse work

Four-week-old male BALB/c nude mice were purchased from Beijing Vital River Laboratory Animal Technology Co., Ltd. (China). All procedures for the animal experiments were conducted according to the Animal Ethics Committee of Tianjin Medical University Cancer Institute & Hospital. All the 14 animals were randomly divided into two groups of 7 mice each. At 5 weeks of age, LC Glc-82 cells (2×10^7/mL) were inoculated subcutaneously into the right flank of 14 mice using 1-ml needles. Two weeks later, when the tumor was visible by the naked eye, the mice were perorally (p.o.) gavaged with either 200 μL normal saline (control) or MHD (300 mg/kg weight), and the animals were gavaged once a day during the experiments. Meanwhile, the tumor volumes were also measured once daily using the following formula: long diameter × (short diameter)^2/2. On day 12, mice were sacrificed and the tumor tissues were weighed. None of mice died during the experiments.

Immunohistochemistry assays

The slides of tumor tissue sections were disposed of deparaffinization and antigen unmasking, and were then incubated with the antibody against Ki-67 (Abcam, UK) at 4°C overnight. After washing with PBS, the slides were incubated with Polymer Helper and Poly peroxidase-anti-mouse/rabbit IgG (PV-9000, ORIGENE, China), followed by further incubation with diaminobenzidine (DAB).

Cellular functional and mechanism assays

The cytotoxicity was assessed by using the instrument of xCELLigence RTCA. Measurements were taken continuously for 72 hours at 37°C, and the RTCA software was used for subsequent data analysis. The cell viability and colony formation assays were carried out as before [19, 20]. The accumulated distance of cells were acquired on the Operetta CLS High Content Analysis System equipped with Harmony software (PerkinElmer, Waltham, MA, USA) using a ×20 long wide distance objective in a digital phase contrast mode at a temperature of 37°C and 5% CO_2. Apoptosis detection, cell cycle assay and western blot (WB) analyses were performed according to the manufacturer's instructions.

Statistical analysis

All data were analyzed using SPSS 17.0 software (USA). Results were represented as mean with standard deviations (mean ± SD). The differences expressed were using the Student's *t*-test, and $P < 0.05$ was considered as statistically significant.

Results

Candidate active ingredients and putative drug targets screening for MHD

To explore the action mechanism of MHD, we first conducted a virtual screening with combined OB and DL, two important ADME parameters, to identify the active ingredients in MHD. Eighteen potential ingredients with OB ≥ 30% and DL ≥ 0.18 from the herb constituents of MHD were obtained. Meanwhile, another 35 ingredients that either exhibit good pharmacological activities (with OB < 30% or DL < 0.18) or have been reported to be typical ingredients of MHD by literature mining were also collected for subsequent analysis. As such, a total of 53 ingredients from the four herbs in MHD were considered as the "candidate ingredients". As shown in **Table 1**, the four herbs, namely MH, GZ, XR and GC contributed 20, 12, 10 and 11 candidate ingredients, respectively.

In some cases, CHM formula shows advantages in treating obscure and complicated disease, such as cancer, due to the synergistic effects among its multiple ingredients and their corresponding targets [21]. Thus, we next explored the putative targets of above 53 candidate ingredients in MHD using TCMSP and SwissTarget Prediction databases, which resulted in a total of 189 putative targets (**Figure 1B**). The numbers of putative targets in MH, GZ, XR and GC were 128, 86, 44 and 66, respectively (**Figure 1C**). Among these herbs, MH had more corresponding targets than the

Table 1. The main potential active ingredients identified by in four herbs

Herbs	Number	Components
Ephedrae Herba (Mahuang)	20	Leucopelargonidin, Quercetin, Delphinidin, Resivit, Kaempferol, Herbacetin, L-ephedrine, D-pseudoephedrine, L-norephedrine, D-norpseudoephedrine, L-methylephedrine, D-methylp-seudoephedrine, Apigenin, Mahuannin A, Ephedrannin A, (+)-Catechin, Benzoic acid, Ferulic acid, Vanillic acid, Ephedran A
Cinnamomi Ramulus (Guizhi)	12	(+)-Catechin, Sitosterol, Beta-sitosterol, ent-Epicatechin, (-)-Taxifolin, Cinnamaldehyde, Cinnamic alcohol, O-Methoxycinnamaldehyde, Cinnamic acid, D-Camphene, ()-Terpinen-4-ol, Benzaldehyde
Armeniacae Semen Amarum (Xingren)	10	Amygdalin, Arachidic acid, Citral, Hexadecanoic acid, Linolenic acid, Mandelonitrile, Myristic acid, Stearic acid, Prunasin, (e)-2-Nonenal
Glycyrrhizae Radix Et Rhizoma (Gancao)	11	Glycyrrhizin, 18Beta-glycyrrhetinic acid, Liquiritigenin, Isoliquiritigenin, Glabridin, Licochalcone A, Liquiritin, Isoliquiritin, Glycyrol, Isoglycyrol, Glabrene

others, indicating it plays an important role in delivering pharmacological activities of MHD. Detailed information of these drug-related targets were listed in Supplementary Table 1. Of note, there were many overlapped targets among different ingredients, suggesting these ingredients may play important role in manifesting synergistic effects of MHD. In addition, the individual drug-target network was constructed to visualize the systematic interactions among these ingredients and their putative targets using Cytoscape 3.2.1 (Supplementary Figure 1).

KEGG enrichment analysis of the putative targets for MHD

Having identified the putative targets of MHD, we performed a KEGG enrichment analysis for these 189 targets using DAVID v6.8. Intriguingly, among the affected signals by MHD, the most enriched signaling pathway was Pathways in cancer, which for the first time suggested a potential application of MHD on cancer treatment (**Figure 1D**). To further evaluate the new use of MHD, the putative drug targets were also enriched in the representative diseases using DAVID v6.8. The result showed that cancer was indeed among the top diseases that could be potentially treated by MHD (Supplementary Figure 2).

Construction of PPI systematic networks and enrichment analysis of the core targets of MHD against LC

Since the curative effect of MHD on respiratory diseases has been well recognized, we then set about to explore the action mechanism of MHD on LC. Four gene expression datasets (GSE22863, GSE27262, GSE43458 and GSE101929) derived from human LC and adjacent normal tissues were obtained from Gene Expression Omnibus (GEO) database. The overlapped 155 disease targets among these datasets were collected as the "LC-related targets" for further analysis (**Figure 2A-C**). Detailed information of these LC-related targets was listed in Supplementary Table 2.

To better understand the complex interactions among the targets, we constructed a PPI network of putative drug-related target for MHD, which contains 5056 nodes and 114586 edges, using the Bisogenet, a key plugin for Cytoscape 3.2.1. Also, a LC-related target PPI network, containing 1674 nodes and 25339 edges, was constructed using the same method. Next, to further investigate the pharmacological mechanisms of MHD against LC, we intersected above two networks and thus obtained 1063 nodes and 19877 edges. Referring to a previous method, the score of DC, a topology parameter, for each node in the overlapping network were calculated by using CytoNCA plugin. Based on the score of DC (> 52), a network of significant targets for MHD against LC, containing 252 nodes and 6809 edges, was thereby constructed [22] (**Figure 3** and Supplementary Table 3).

We subsequently performed an enrichment analysis for these identified 252 core targets (nodes in the PPI network) by dividing them into GO biological process and KEGG signaling pathways. Specifically, the enriched biological processes were mainly focused on apoptosis and transcription, while the affected signaling pathways mainly included pathways in cancer, PI3K-Akt signaling pathway, cell cycle, MAPK signaling pathway, Epstein-Barr virus infection

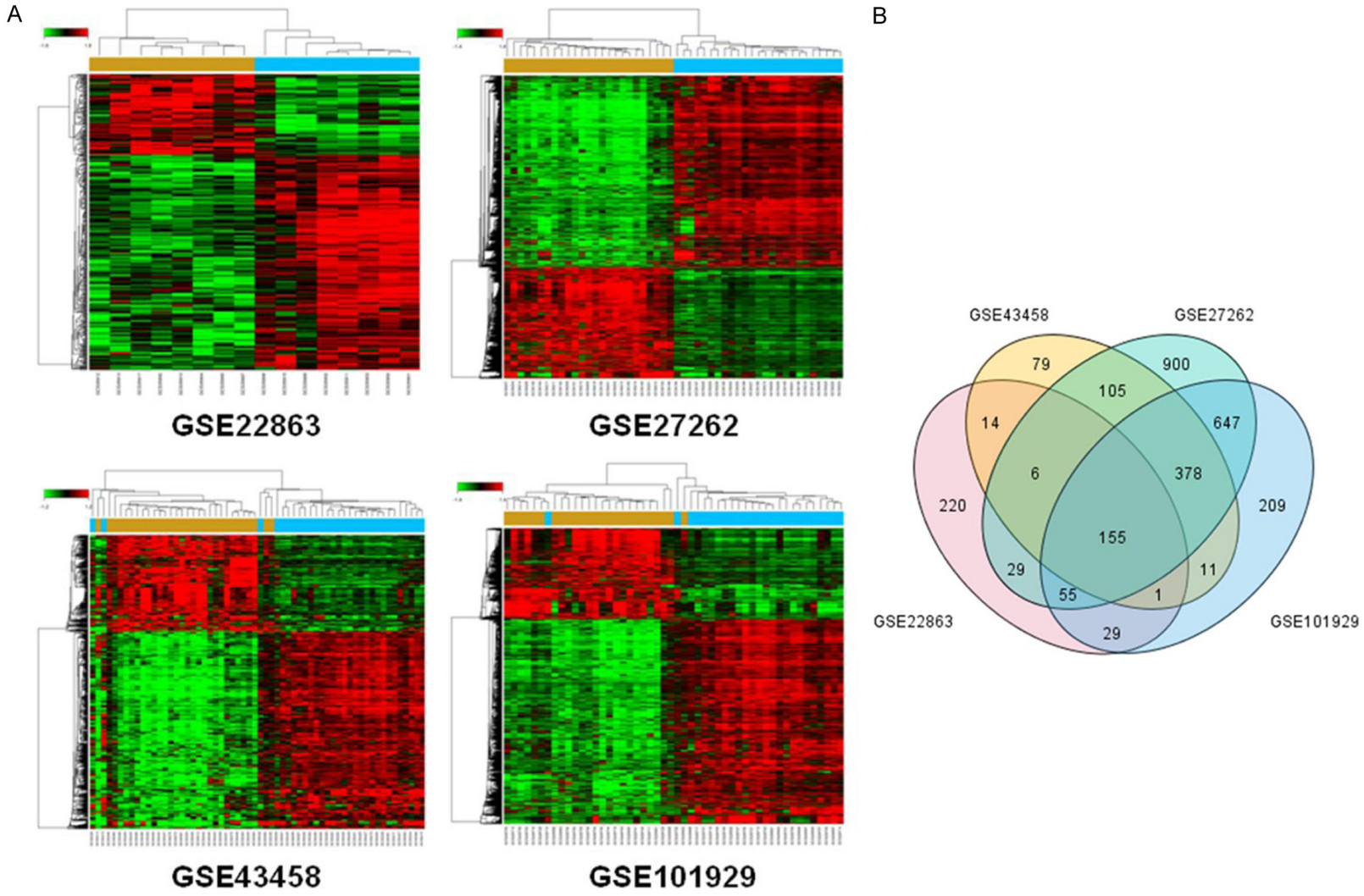
A
GSE22863
GSE27262
GSE43458
GSE101929
B
GSE43458
GSE27262
GSE22863
GSE101929
79
900
105
14
647
6
378
220
209
155
29
11
55
1
29

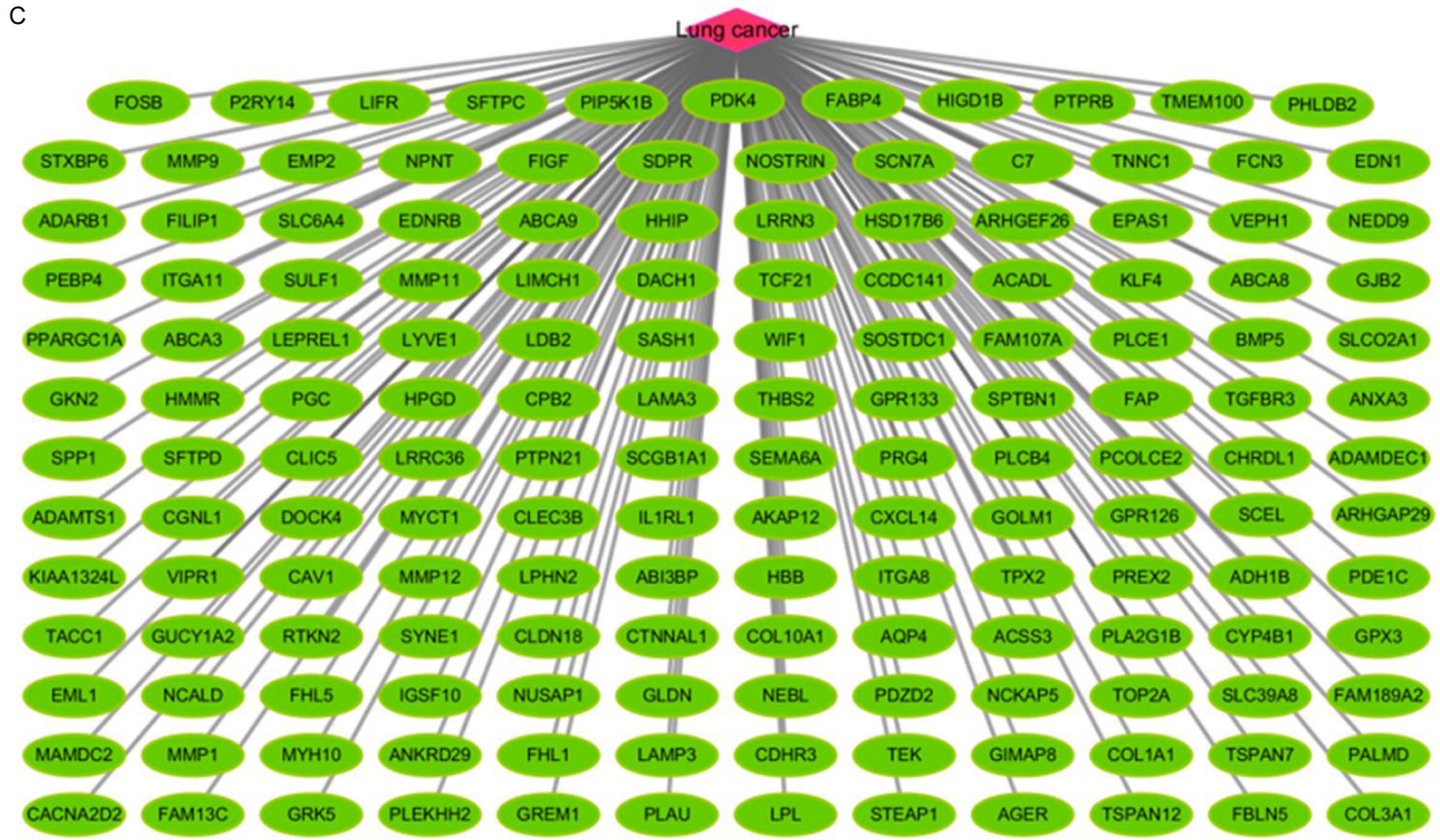

Figure 2. The known LC-related targets were screened from Gene Expression Omnibus (GEO) database. A. Four heat maps from GEO chips, including GSE22863, GSE27262, GSE43458 and GSE101929. B. The Venn diagram of 155 common LC-related targets from 4 GEO chips. C. Construction of the LC-related disease targets network.

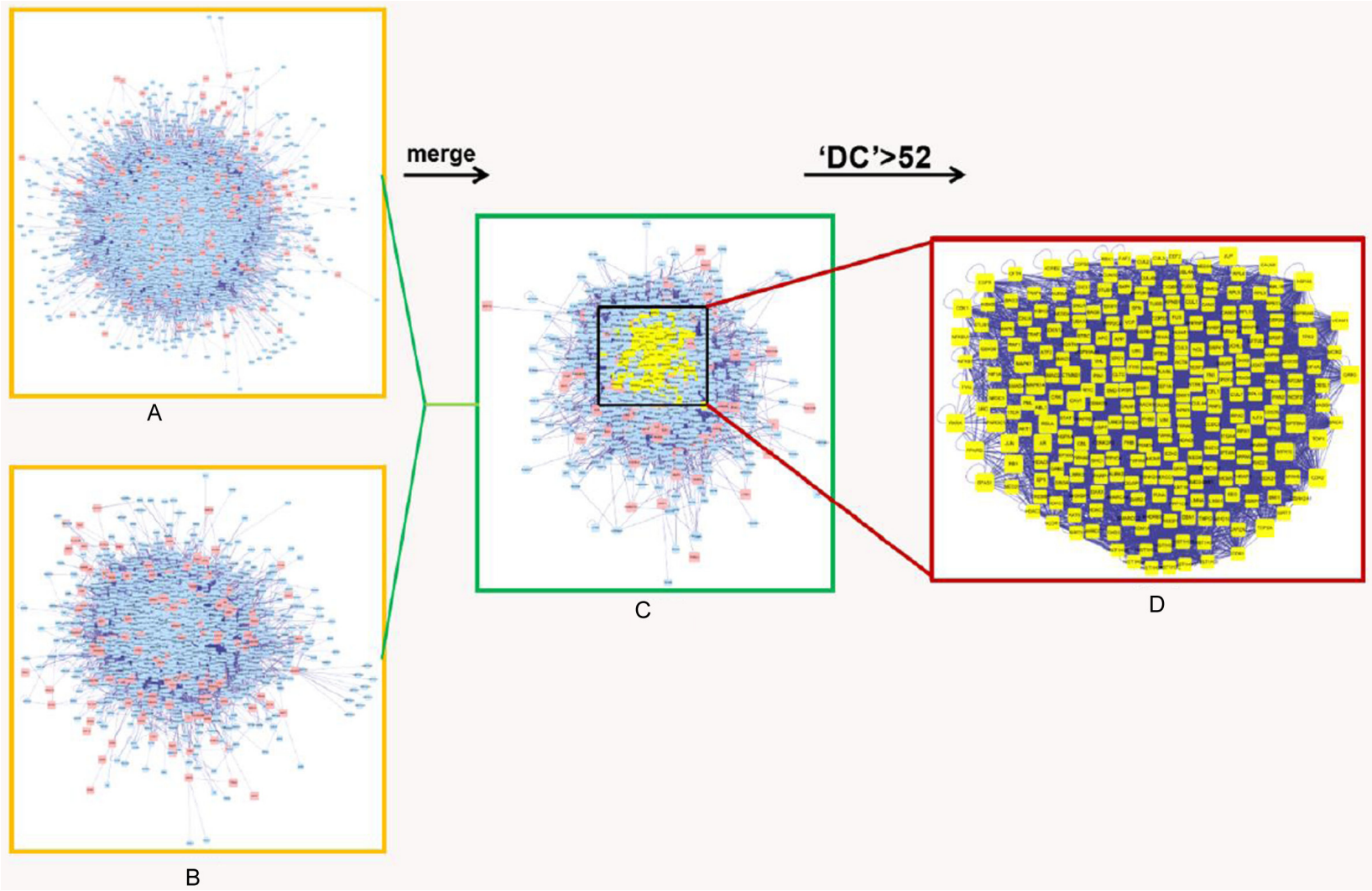

Figure 3. In silico identification and systematic network construction of candidate core targets for MHD against LC. (A) The interactive PPI network of MHD putative drug targets was made of 5056 nodes and 114586 edges. (B) The interactive PPI network of LC-related disease targets was composed of 1674 nodes and 25339 edges. (C) The interactive PPI network of MHD against GC-related targets made of 1063 nodes and 19877 edges was shown. (D) PPI network of core targets extracted from (C), in which 252 nodes and 6809 edges were included.

and viral carcinogenesis (**Figure 4A**, **4B** and **Tables 2**, **3**). These results indicated that MHD is likely to inhibit the growth of LC cells by regulating the key signaling pathways involving cell proliferation, apoptosis and cell cycle.

MHD inhibited LC growth in vivo and decreased the viability and motility of LC cells in intro

To investigate the direct cancer suppressive role of MHD *in vivo*, we determined the effect of MHD on xenografted LC on immunodeficient mice. As shown in **Figure 5A** and **5B**, compared with the control mice, the growth of xenografted LC was greatly suppressed by MHD treatment. By day 12, the tumor volume of MHD-treated group were approximately 2.8-fold smaller than that of control group ($P < 0.05$) (**Figure 5C**). In line with this, the tumor weights showed a striking difference between the two groups ($P < 0.05$) (**Figure 5D**). The subsequent immunohistochemistry analysis showed that the number of Ki-67 positive cells was significantly decreased in MHD-treated tumors, compared to those in controls, indicating an anti-proliferative effect of MHD on these tumors (**Figure 5E**, **5F**). These results provided an convincing evidence showing that MHD possesses a direct anti-LC activity.

Next, we further evaluate the growth suppressive effect of MHD on LC cells using xCELLigence RTCA instrument. The results from dynamic monitor of the cytoactivity revealed that the growth ability of LTEP-A-2 and Glc-82 LC cells were dramatically suppressed in MHD treatment group in a dose-dependent manner, compared to that in the control group (**Figure 6A**, **6B**). Meanwhile, the results of CCK-8 assay showed that the viability of LC cells was significantly inhibited by MHD in a dose-dependent manner (**Figure 6C**, **6D**). After treating the cells for 24 hours, IC_{50} analyses showed that MHD exerted its 50% inhibitory effect on LTEP-A-2 cells at 173.40±4.89 μg/mL and Glc-82 cells at 278.90±4.30 μg/mL, respectively.

Furthermore, the ability of cell colony formation of the LC cells was determined in the presence of MHD. The results showed that the cell clonality of the LC cells was decreased in a dose-dependent manner following MHD treatment for 24 hours (**Figure 6E-H**). In addition, the average of accumulated distance of the migrating population in MHD treatment cells was also smaller than that of control cells, indicating that the cell mobility was inhibited by MHD treatment (**Figure 6I-N**). Thus, the above results demonstrated a direct inhibitory effect of MHD on the viability and motility of LC cells *in vitro*.

MHD induced apoptosis and cell cycle arrest of LC cells

We next carried out a serial of cellular functional assays to validate the *in silico* enrichment analysis results above. Firstly, the morphology of LC cells was observed after MHD treatment for 24 hours. Compared to the control cells, the MHD-treated cells showed typical characteristics of cell apoptosis, such as shrinkage, roundness and disappearance of stereopsis. Meanwhile, the MHD-treated cell nucleus showed dense Hoechst 33342 staining by fluorescence observation (**Figure 7A**). Also, the flow cytometry analysis revealed that the apoptotic population stained with Annexin V-FITC was significantly increased upon MHD treatment in a dose-dependent manner (**Figure 7B-D**). The following WB results also demonstrated that MHD promoted the accumulation of pro-apoptosis proteins Bax and cleaved Caspase-9, whereas the level of anti-apoptosis protein Bcl-2 was down-regulated by MHD in a dose-dependent manner (**Figure 7H** and Supplementary Figure 4A).

Furthermore, we performed BrdU-incorporated cell profiling assay to evaluate the effect of MHD treatment on LC cell cycle. The results showed that MHD treatment significantly inhibited the proliferation rate of LC cells by arresting them at S phase (**Figure 7E-G**). Consistently, accumulation of the S phase-specific marker Cyclin A2 and down-regulated Cyclin D1, CDK 2 and Cyclin B1 protein levels were observed in the MHD-treated LC cells (**Figure 7H** and Supplementary Figure 4A). Together, these results showed that MHD inhibited cell growth via inducing cell cycle arrest and apoptosis of LC cells.

MHD inhibited growth of LC cells through impeding Akt/ERK signaling pathways

To further explore the underlying mechanism of the inhibitory effect of MHD on the growth of

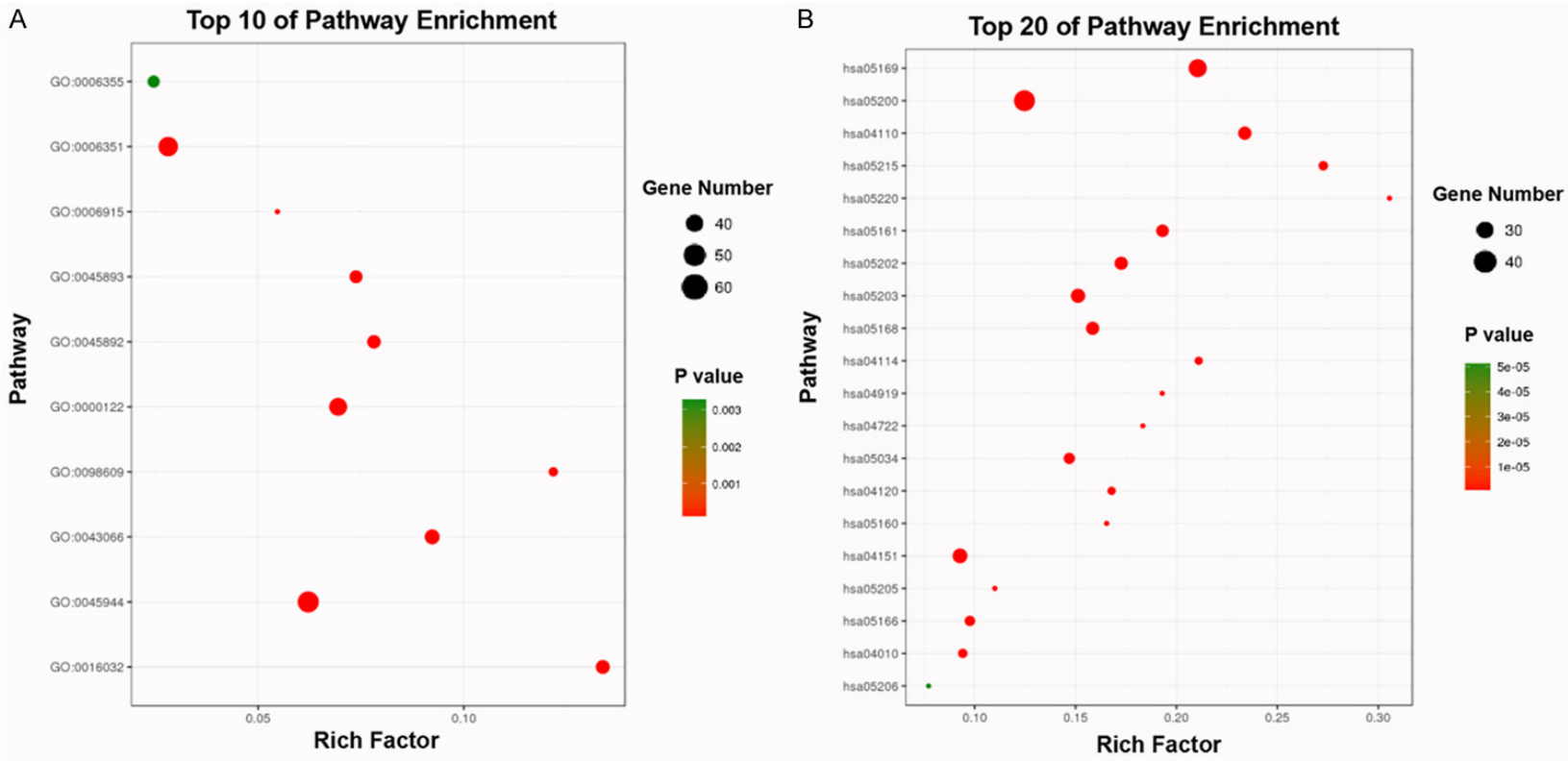

Figure 4. GO and KEGG enrichment analysis of candidate core targets for MHD against LC. A. Candidate core targets were enriched in the representative biological processes (GO-BP) by using DAVID v6.8 (p-value < 0.05). B. Candidate core targets were enriched in the representative signaling pathways (KEGG) by using DAVID v6.8 (p-value < 0.05).

Table 2. GO enrichment analysis of potential core targets for MHD against LC

Term	Gene count	*P*-value
GO-BP:0045944~positive regulation of transcription from RNA polymerase II promoter	61	1.73E-21
GO-BP:0006351~transcription, DNA-templated	55	5.17E-06
GO-BP:0000122~negative regulation of transcription from RNA polymerase II promoter	50	1.96E-19
GO-BP:0043066~negative regulation of apoptotic process	42	1.06E-20
GO-BP:0016032~viral process	40	1.38E-25
GO-BP:0045892~negative regulation of transcription, DNA-templated	39	8.99E-17
GO-BP:0045893~positive regulation of transcription, DNA-templated	38	1.84E-15
GO-BP:0006355~regulation of transcription, DNA-templated	37	0.00321423
GO-BP:0098609~cell-cell adhesion	33	8.60E-20
GO-BP:0006915~apoptotic process	31	1.90E-09

Table 3. KEGG enrichment analysis of potential core targets for MHD against LC

Term	Gene count	*P*-value
hsa05200:Pathways in cancer	49	7.22E-19
hsa05169:Epstein-Barr virus infection	40	1.42E-23
hsa04151:PI3K-Akt signaling pathway	32	7.35E-09
hsa05203:Viral carcinogenesis	31	5.50E-14
hsa04110:Cell cycle	29	3.03E-18
hsa05202:Transcriptional misregulation in cancer	29	1.42E-14
hsa05168:Herpes simplex infection	29	1.32E-13
hsa05161:Hepatitis B	28	2.43E-15
hsa05034:Alcoholism	26	1.87E-11
hsa05166:HTLV-I infection	25	2.00E-07
hsa05215:Prostate cancer	24	1.16E-16
hsa04010:MAPK signaling pathway	24	7.24E-07
hsa04114:Oocyte meiosis	23	2.00E-13
hsa04120:Ubiquitin mediated proteolysis	23	2.51E-11
hsa05220:Chronic myeloid leukemia	22	2.27E-16
hsa04919:Thyroid hormone signaling pathway	22	4.76E-12
hsa04722:Neurotrophin signaling pathway	22	1.34E-11
hsa05160:Hepatitis C	22	1.02E-10
hsa05205:Proteoglycans in cancer	22	1.81E-07
hsa05206:MicroRNAs in cancer	22	5.15E-05

LC cells, we next evaluated the activities of the key signaling pathways involving cell proliferation and viability. Among those, PI3K-Akt and MAPK signaling pathways were selected for further investigation based on the previous KEGG pathway enrichment analysis. Indeed, these pathways were significantly impeded by MHD treatment, evidenced by dramatically reduced levels of the key factors in these pathways, such as p-Akt (S473) and p-ERK (T202/Y204). Furthermore, the levels of pan-Akt and pan-ERK were also down-regulated by MHD treatment (**Figure 8** and Supplementary Figure 4B). Therefore, these results indicated that the affected apoptosis and proliferation of LC cells by MHD treatment were likely resulted from simultaneous inhibition of Akt/ERK signaling pathways, which shows a typical "multi-ingredient, multi-target and multi-function" pharmacological characteristics of CHM.

Discussion

Syndrome differentiation is the core principle in TCM clinical practice, and the treatment protocol for the patient is guided by the TCM syndrome instead of the specific disease defined by modern medicine. However, the same TCM syndrome may manifest in different diseases, which means a given CHM formula might be effective on different diseases with the same syndrome. Therefore, to bring the ancient TCM practice into line with the modern medicine, it is an essential step to explore the "new use of old formula". Undoubtedly, to decipher the action mechanism of CHM with a better understanding of the synergistic action among the multiple active ingredients in CHM, and to explore how this synergistic action results in a synergistic effect through their cor-

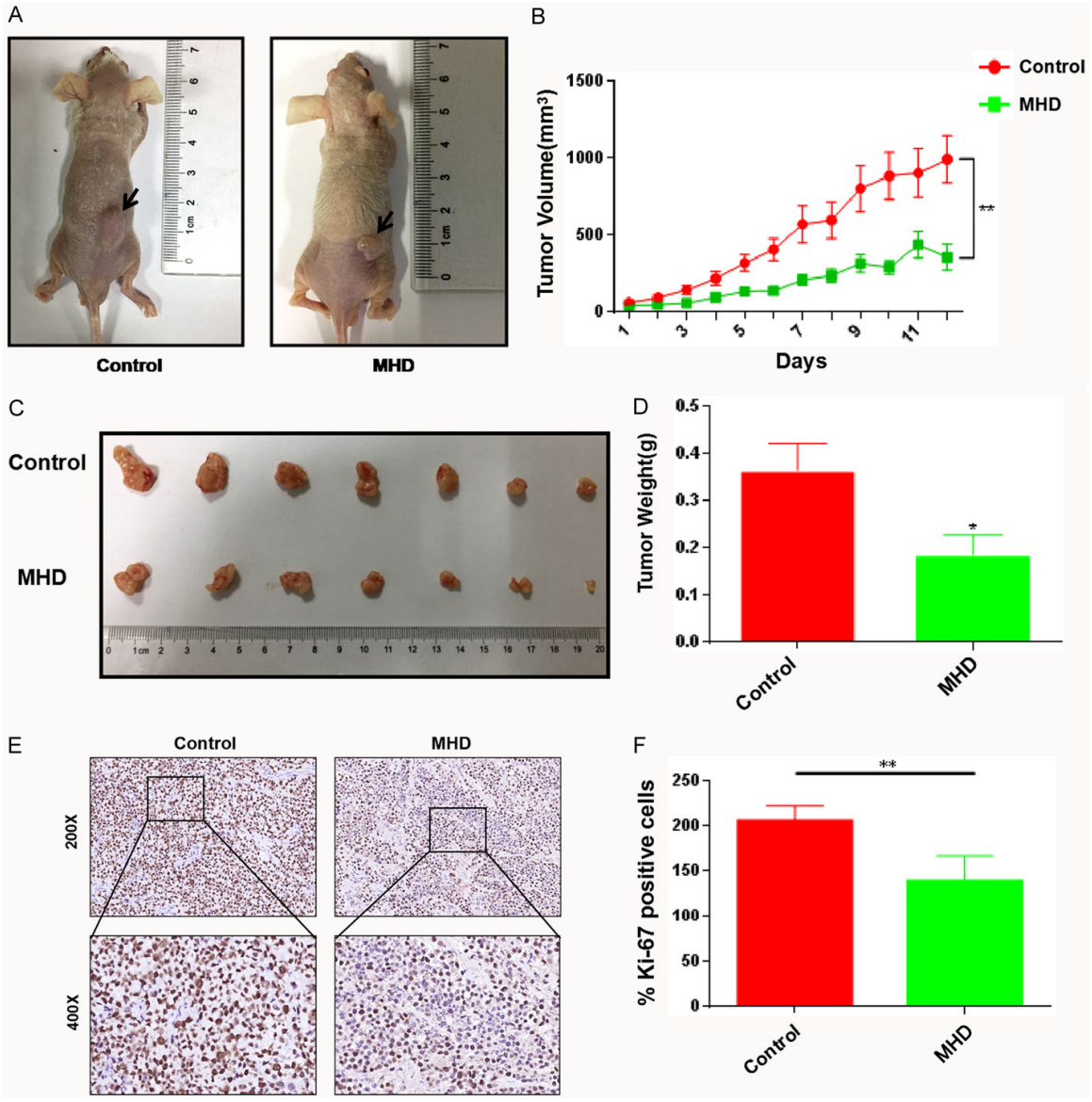

Figure 5. MHD suppressed development of the xenografted LC tumors on mice. A, B. The tumor volumes were measured and calculated once daily for 12 consecutive days. C. The photo of tumor sizes was shown on the day 12. D. The tumors were resected and weighted on the day 12. E. Immunohistochemistry staining for Ki-67 was performed by using the tumor slides from control and MHD-treated groups. F. Statistical analysis of the positive ratio of Ki-67 staining. *P < 0.05 based on the Student t-test.

responding targets, may shed light on the new clinical applications of CHM. However, it is now still a bottleneck to unveil the scientific basis of the action mechanism for a given CHM in a holistic perspective by conventional approaches.

In fact, the holistic view of TCM shares much with the concepts of emerging system biology and network pharmacology, which define the complex and multi-level interactions through systematic analyses of various networks. Based on this point, a novel TCM network pharmacology approach has been recently launched, along with a series of powerful computational tools for TCM research. In this study, we started to explore the action mechanism of MHD by utilizing the TCM network pharmacology and bioinformatics analysis tools, which led to an interesting discovery of a potential pharmacological activity for MHD in cancer treatment. Indeed, the *in vivo* assay demonstrated the significant growth inhibition of xenografted LC cells after oral administration of MHD in immu-

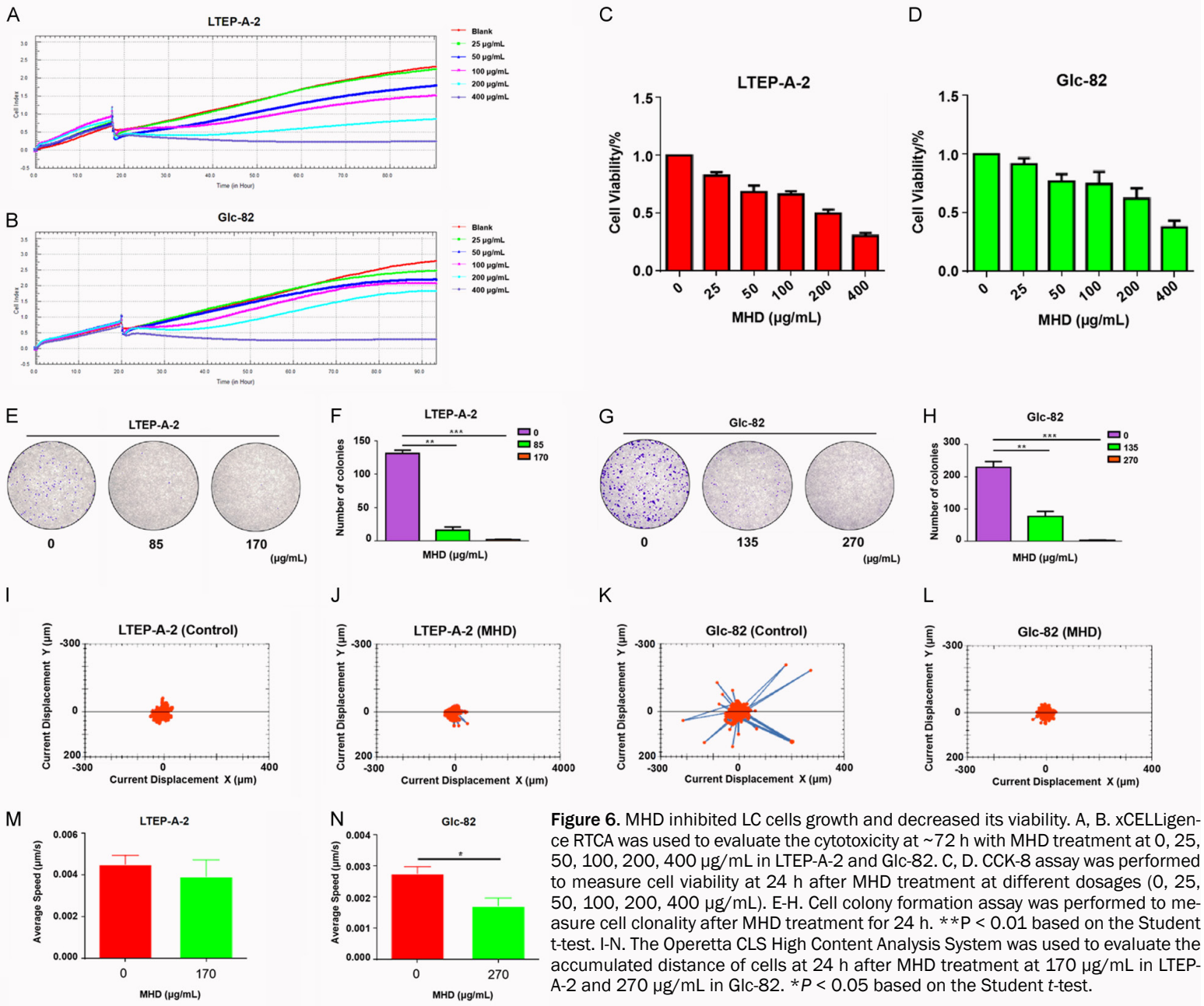

Figure 6. MHD inhibited LC cells growth and decreased its viability. A, B. xCELLigence RTCA was used to evaluate the cytotoxicity at ~72 h with MHD treatment at 0, 25, 50, 100, 200, 400 μg/mL in LTEP-A-2 and Glc-82. C, D. CCK-8 assay was performed to measure cell viability at 24 h after MHD treatment at different dosages (0, 25, 50, 100, 200, 400 μg/mL). E-H. Cell colony formation assay was performed to measure cell clonality after MHD treatment for 24 h. **P < 0.01 based on the Student t-test. I-N. The Operetta CLS High Content Analysis System was used to evaluate the accumulated distance of cells at 24 h after MHD treatment at 170 μg/mL in LTEP-A-2 and 270 μg/mL in Glc-82. *$P < 0.05$ based on the Student *t*-test.

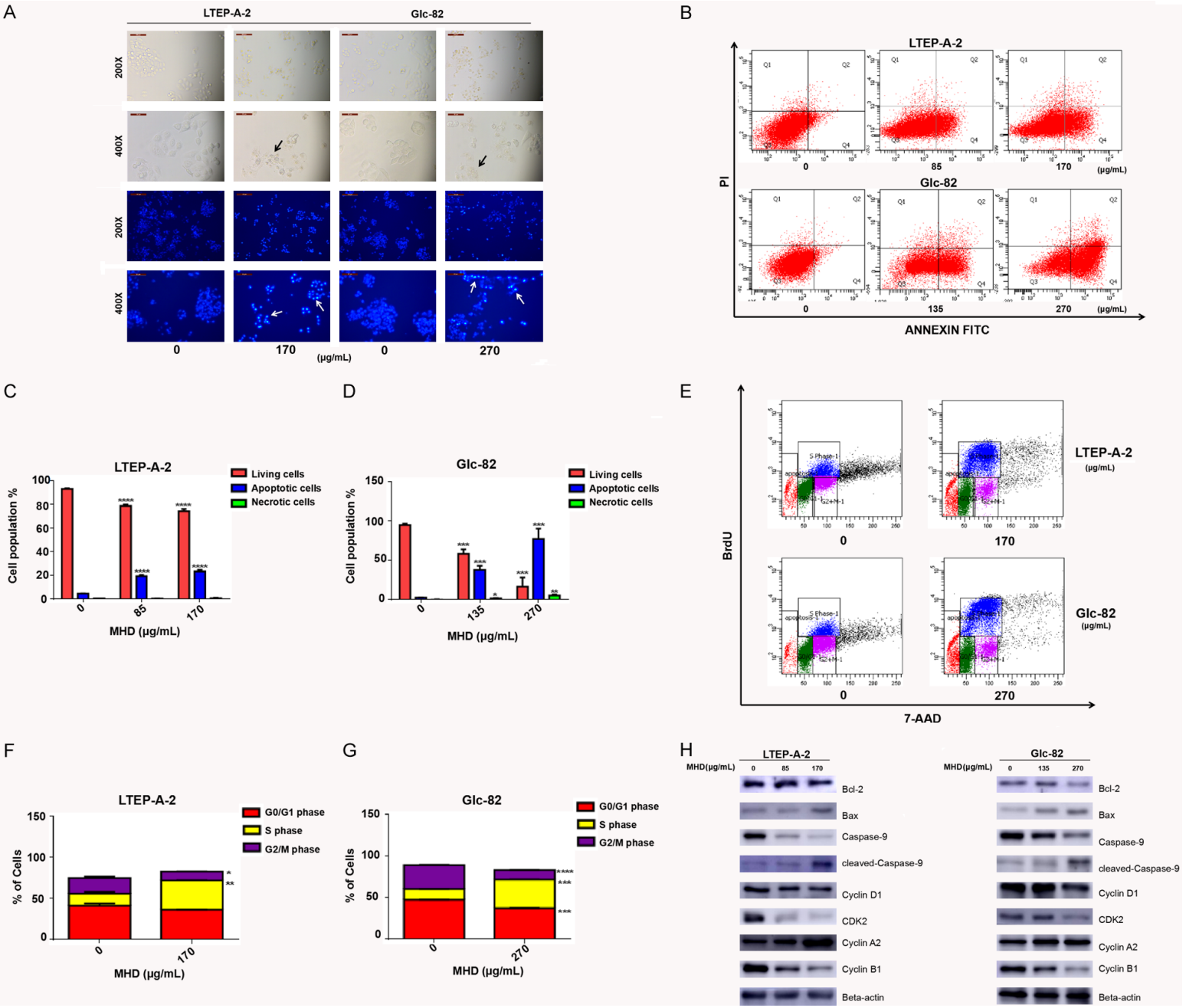
A
LTEP-A-2
Glc-82
200X
400X
200X
400X
0
170
(μg/mL)
0
270
B
LTEP-A-2
PI
0
85
170
(μg/mL)
Glc-82
0
135
270
(μg/mL)
ANNEXIN FITC
C
LTEP-A-2
Cell population %
Living cells
Apoptotic cells
Necrotic cells
MHD (μg/mL)
D
Glc-82
Cell population %
Living cells
Apoptotic cells
Necrotic cells
MHD (μg/mL)
E
BrdU
LTEP-A-2
(μg/mL)
0
170
Glc-82
(μg/mL)
0
270
7-AAD
F
LTEP-A-2
% of Cells
G0/G1 phase
S phase
G2/M phase
MHD (μg/mL)
G
Glc-82
% of Cells
G0/G1 phase
S phase
G2/M phase
MHD (μg/mL)
H
LTEP-A-2
MHD(μg/mL)
0
85
170
Bcl-2
Bax
Caspase-9
cleaved-Caspase-9
Cyclin D1
CDK2
Cyclin A2
Cyclin B1
Beta-actin
Glc-82
MHD(μg/mL)
0
135
270
Bcl-2
Bax
Caspase-9
cleaved-Caspase-9
Cyclin D1
CDK2
Cyclin A2
Cyclin B1
Beta-actin

Figure 7. MHD treatment resulted in apoptosis and disturbance of cell cycle progression in LC cells. A. The cell morphology was observed in white light and fluorescence field using an inverted microscope. B. Induction of apoptosis of LTEP-A-2 and Glc-82 LC cells after MHD treatment. LTEP-A-2 cells were treated with MHD at different concentrations (0, 85 and 170 μg/mL) for 24 h, and Glc-82 cells were also treated with MHD at different concentrations (0, 135 and 270 μg/mL) for 24 h, when apoptotic events was assessed by flow cytometry. C, D. Statistical analysis of the percentages of the apoptotic cells in LTEP-A-2 and Glc-82 cells. **P < 0.01 based on the Student *t*-test. E. Cell cycle analysis of LC cells following MHD treatment in LTEP-A-2 (0 and 170 μg/mL) and Glc-82 (0 and 270 μg/mL) for 24 h by flow cytometry. F, G. Statistical analysis of the proportions of the cells at different phases in LTEP-A-2 and Glc-82 cells. ***P* < 0.01 based on the Student *t*-test. H. LTEP-A-2 (0, 85 and 170 μg/mL) and Glc-82 (0, 135 and 270 μg/mL) cells were treated with MHD at different concentrations for 24 h. After proteins were extracted, the protein expression levels of Bcl-2, Bax, pro-caspase-9, cleaved-caspase-9, Cyclin D1, CDK2, Cyclin A2 and Cyclin B1 were analyzed by WB assay.

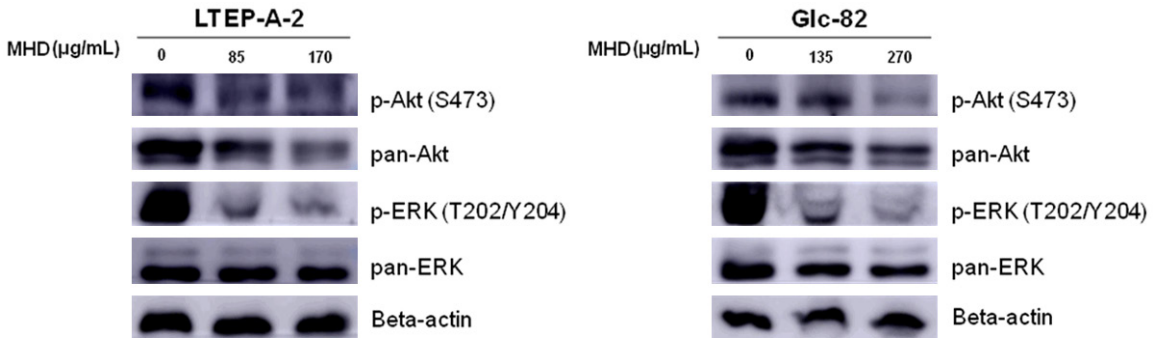

Figure 8. MHD treatment resulted in down-regulating the phosphorylation protein expression level of Akt and ERK signaling pathways. LTEP-A-2 (0, 85 and 170 μg/mL) and Glc-82 (0, 135 and 270 μg/mL) cells were treated with MHD at different concentrations for 24 h. After proteins were extracted, the expression levels of p-Akt (S473), pan-Akt, p-ERK (T202/Y204) and pan-ERK were analyzed by WB assay.

nodeficient mice. To further explore the underlying mechanism by untangling the complex interactions among the targets, we constructed a integrative PPI network based on the MHD-related and LC-related networks. According to the topo-parameter DC in the network, a total of 252 core targets were thereby identified to involve in the pharmacological effect of MHD against LC.

The subsequent GO and KEGG signaling pathway enrichment analyses for these core targets showed that apoptosis and transcription are the most affected biological processes by MHD treatment, while the disturbed signaling pathways mainly includes pathways in cancer, PI3K-Akt signaling pathway, and MAPK signaling pathway, suggesting that the inhibitory effect of MHD on LC cells is likely resulted from disturbance of the key signaling pathways involving in apoptosis and cell proliferation. Indeed, our western blot results showed that the levels of p-Akt (S473) and p-ERK (T202/Y204) were both dramatically reduced upon MHD treatment in LC cells. These results are in line with those of previous studies, which showed the anti-cancer effects of multiple ingredients from the herbs contained in MHD. For instance, cinnamic acid, a key ingredient from *Cinnamomi Ramulus* (GZ), could induce cell apoptosis and decrease the proliferation rate of melanoma cells, while its derivatives induced apoptotic cell death in colon and cervical cancer cells [23, 24]. Amygdalin, an ingredient contained in *Semen Amarum* (XR), has been reported to exhibit its cytotoxic effect on multiple solid tumors by inhibiting cell proliferation, inducing cell apoptosis and impairing the immune functions *in vivo* [25]. Furthermore, several studies have previously determined the association between the ingredients identified in the present study and the key signaling pathways affected by MHD treatment. For example, cinnamaldehyde, another ingredient from GZ, exhibited desirable pharmacological activities in inhibiting angiogenesis and metastasis of tumor cells by targeting PI3K/Akt pathway [26]. Similarly, herbacetin, an ingredient of *Ephedrae herba* (MH), could suppress the motility of breast cancer cells by

impeding the same pathway [27]. Also, glycyrrhizin from *Glycyrrhizae Radix Et Rhizoma* (GC) suppressed the growth and migration of leukemia cell via blocking Akt/mTOR signalings [28]. Meanwhile, 18β-glycyrrhetinic acid, an ingredient from *Glycyrrhizae Radix Et Rhizoma* (GC), was found to suppress the cell porliferation through inhibiting ERK signaling pathway in NSCLC cells [29]. Together, these results support a view that MHD holds a promising potential with its multi-component, multi-targets, multi-levels and coordinated intervention effects on LC treatment (Supplementary Figure 3).

Acknowledgements

We are grateful to Prof. Hongbin Liu for his valuable suggestions on this study. This study was funded by the National Natural Science Foundation of China (No. 81572416 and No. 81703454), the National Key Technologies R&D Program of China (No. 2016YFC1303-200), and the Tianjin Medical University Cancer Institute & Hospital Cancer Translational Medicine Seed Funds (No. 1701-1). The protocol for animal experimentation has been approved by the Institution Animal Care of Tianjin Medical University Cancer Institute & Hospital.

Disclosure of conflict of interest

None.

Abbreviations

LC, Lung cancer; MHD, Mahuang Decoction; CHM, Chinese herb medicine; TCM, Traditional Chinese medicine; FBS, Fetal bovine serum; CCK-8, Cell counting kit-8; OB, Oral bioavailability; DL, Drug-likeness; PPI, Protein-protein interaction; DC, Degree centrality.

Address correspondence to: Liren Liu, Department of Gastrointestinal Cancer Biology, Tianjin Medical University Cancer Institute and Hospital, Tianjin 300060, China; National Clinical Research Center of Cancer, Huanhuxi Road, Hexi District, Tianjin 300060, China. Tel: +86-22-23340123; E-mail: liuliren@tmu.edu.cn

References

[1] Wistuba I, Gelovani J, Jacoby J, Davis S and Herbst R. Methodological and practical challenges for personalized cancer therapies. Nat Rev Clin Oncol 2011; 8: 135-141.

[2] Yang P, Allen M and Aubry M. Clinical features of 5,628 primary lung cancer patients: experience at Mayo Clinic from 1997 to 2003. Chest 2005; 128: 452-462.

[3] Cao M and Chen W. Epidemiology of lung cancer in China. Thorac Cancer 2019; 10: 3-7.

[4] Doroshow D and Herbst R. Treatment of advanced non-small cell lung cancer in 2018. JAMA Oncol 2018; 4: 569-570.

[5] Tang J, Liu B and Ma K. Traditional Chinese medicine. Lancet 2008; 372: 1938-1940.

[6] Zhao L, Wang J, Li H, Che J, Ma N and Cao B. Safety and efficacy of tianfoshen oral liquid in non-small cell lung cancer patients as an adjuvant therapy. Evid Based Complement Alternat Med 2019; 2019: 1375439.

[7] Sun X, Xu X, Chen Y, Guan R, Cheng T, Wang Y, Jin R, Song M and Hang T. Danggui buxue decoction sensitizes the response of non-small-cell lung cancer to gemcitabine via regulating deoxycytidine kinase and P-glycoprotein. Molecules 2019; 24: E2011.

[8] Kuo Y, Liao H, Chiang J, Wu M, Chen B, Chang C, Yeh M, Chang T, Sun M, Yeh C and Yen H. Complementary chinese herbal medicine therapy improves survival of patients with pancreatic cancer in taiwan: a nationwide population-based cohort study. Integr Cancer Ther 2018; 17: 411-422.

[9] He Y, Lou X, Jin Z, Yu L, Deng L and Wan H. Mahuang decoction mitigates airway inflammation and regulates IL-21/STAT3 signaling pathway in rat asthma model. J Ethnopharmacol 2018; 224: 373-380.

[10] Wan J, Tian Y, Wan H, Yu L, Zhou H, Li C and He Y. Pharmacokinetics of compatible effective components of Mahuang Decoction in febrile rats. Zhongguo Zhong Yao Za Zhi 2019; 44: 2149-2155.

[11] Huang S, Tong H and Ye S. Clinical observation on shegan mahuang tang in treating chronic cough after radical lung cancer surgery. Zhejiang Chinese Medical University Xue Bao 2012; 36: 398.

[12] Zhang J and Wu Y. Observation on the therapeutic effect of Fufang Shengmahuang decoction on malignant pleural effusion in 68 patients with non-small cell lung cancer (NSCLC). China Journal of Pharmaceutical Economics 2012; 3: 246-248.

[13] Pei T, Zheng C, Huang C, Chen X, Guo Z, Fu Y, Liu J and Wang Y. Systematic understanding the mechanisms of vitiligo pathogenesis and its treatment by qubaibabuqi formula. J Ethnopharmacol 2016; 190: 272-287.

[14] Zhang W, Tao Q, Guo Z, Fu Y, Chen X, Shar P, Shahen M, Zhu J, Xue J, Bai Y, Wu Z, Wang Z,

Xiao W and Wang Y. Systems pharmacology dissection of the integrated treatment for cardiovascular and gastrointestinal disorders by traditional Chinese medicine. Sci Rep 2016; 6: 32400.
[15] Yu H, Chen J, Xu X, Li Y, Zhao H, Fang Y, Li X, Zhou W, Wang W and Wang Y. A systematic prediction of multiple drug-target interactions from chemical, genomic, and pharmacological data. PLoS One 2012; 7: e37608.
[16] Shannon P, Markiel A, Ozier O, Baliga N, Wang J, Ramage D, Amin N, Schwikowski B and Ideker T. Cytoscape: a software environment for integrated models of biomolecular interaction networks. Genome Res 2003; 13: 2498-2504.
[17] Huang D, Sherman B and Lempicki R. Systematic and integrative analysis of large gene lists using DAVID bioinformatics resources. Nat Protoc 2009; 4: 44-57.
[18] Huang D, Sherman B and Lempicki R. Bioinformatics enrichment tools: paths toward the comprehensive functional analysis of large gene lists. Nucleic Acids Res 2009; 37: 1-13.
[19] Pan B, Zang J, He J, Wang Z and Liu L. Add-on therapy with Chinese herb medicine Bo-Er-Ning capsule (BENC) improves outcomes of gastric cancer patients: a randomized clinical trial followed with bioinformatics-assisted mechanism study. Am J Cancer Res 2018; 8: 1090-1105.
[20] Pan B, Shi X, Ding T and Liu L. Unraveling the action mechanism of polygonum cuspidatum by a network pharmacology approach. Am J Transl Res 2019; 11: 6790-6811.
[21] Li S and Zhang B. Traditional Chinese medicine network pharmacology: theory, methodology and application. Chin J Nat Med 2013; 11: 110-120.
[22] Butler M, Robertson A and Cooper M. Natural product and natural product derived drugs in clinical trials. Nat Prod Rep 2014; 31: 1612-1661.
[23] Niero E and Machado-Santelli G. Cinnamic acid induces apoptotic cell death and cytoskeleton disruption in human melanoma cells. J Exp Clin Cancer Res 2013; 32: 31.
[24] Anantharaju P, Reddy D, Padukudru M, Kumari Chitturi C, Vimalambike M and Madhunapantula S. Induction of colon and cervical cancer cell death by cinnamic acid derivatives is mediated through the inhibition of histone deacetylases (HDAC). PLoS One 2017; 12: e0186208.
[25] Shi J, Chen Q, Xu M, Xia Q, Zheng T, Teng J, Li M and Fan L. Recent updates and future perspectives about amygdalin as a potential anticancer agent: a review. Cancer Med 2019; 8: 3004-3011.
[26] Patra K, Jana S, Sarkar A, Mandal D and Bhattacharjee S. The inhibition of hypoxia-induced angiogenesis and metastasis by cinnamaldehyde is mediated by decreasing HIF-1α protein synthesis via PI3K/Akt pathway. Biofactors 2019; 45: 401-415.
[27] Hyuga S, Hyuga M, Yoshimura M, Amakura Y, Goda Y and Hanawa T. Herbacetin, a constituent of ephedrae herba, suppresses the HGF-induced motility of human breast cancer MDA-MB-231 cells by inhibiting c-Met and Akt phosphorylation. Planta Med 2013; 79: 1525-1530.
[28] He S, Gao M, Fu Y and Zhang Y. Glycyrrhizic acid inhibits leukemia cell growth and migration via blocking AKT/mTOR/STAT3 signaling. Int J Clin Exp Pathol 2015; 8: 5175-5181.
[29] Huang R, Chu Y, Huang Q, Chen X, Jiang Z, Zhang X and Zeng X. 18β-glycyrrhetinic acid suppresses cell proliferation through inhibiting thromboxane synthase in non-small cell lung cancer. PLoS One 2014; 9: e93690.

Supplementary Table 1. MHD-related targets

MHD-related targets
ABCB1
ABCC1
ACACA
ACHE
ACPP
ADH1A
ADH1B
ADH1C
ADH4
ADH7
ADORA1
ADRA1A
ADRA1B
ADRA1D
ADRA2A
ADRA2B
ADRA2C
ADRB1
ADRB2
AHR
AKR1A1
AKR1B1
AKR1C3
ALOX5
AR
BACE1
BCHE
BCL2
C5AR1
CA1
CA2
CALM1
CAT
CCL2
CCNA2
CDK1
CDK2
CDK4
CDK6
CHEK1
CHRM1
CHRM2
CHRM3
CHRM4
CHRNA2
CHRNA7
COL1A1

COL3A1
CRYZ
CTNNA1
CTNNB1
CTRB1
CTSD
CYP19A1
CYP1A2
CYP2B6
CYP2E1
CYP3A4
DAO
DCT
DPP4
DRD1
EGF
EGFR
ESR1
ESR2
F10
F2
F3
F7
FASN
GABRA1
GABRA2
GABRA3
GABRA5
GABRA6
GJA1
GLI1
GSK3B
GSTM1
GSTM2
GSTP1
HMOX1
HSD11B1
HSD11B2
HSP90AB1
HSPA5
HTR1A
HTR2A
IFNB1
IFNG
IGHG1
IL1B
IL2
IL6
INS

INSR
IRF3
JAK2
JUN
JUP
KCNH2
KCNMA1
KDR
LTA4H
MAOA
MAOB
MAP2
MAPK1
MAPK14
MAPK8
MAPT
MBNL1
MED6
MGAM
MMP1
MMP2
MMP3
MPO
MS4A2
NCOA1
NCOA2
NFE2L2
NFKBIA
NOS2
NOS3
NQO1
NR3C1
NR3C2
ODC1
OPRM1
PCYT1A
PDE3A
PDE5A
PGR
PIK3CG
PIM1
PKIA
PLA2G2A
PLA2G2E
PLAT
PLAU
PON1
POR
PPARG

PPP3CA
PRKACA
PRSS1
PRSS3
PTGER3
PTGS1
PTGS2
PTPN1
RB1
RELA
RHO
RPS6KA4
RXRA
RXRB
SCN5A
SELE
SERPINC1
SERPIND1
SLC16A7
SLC28A1
SLC5A1
SLC6A2
SLC6A3
SLC6A4
SOD1
SULT1E1
TDP1
THBD
TLR4
TNF
TOP1
TOP2A
TP53
TRPA1
TRPV1
TRPV4
TXNRD1
TYR
TYRP1
VCAM1
VEGFA
VKORC1
VPS29
XDH

Supplementary Table 2. LC-related targets

LC-related targets
ABCA3
ABCA8
ABCA9
ABI3BP
ACADL
ACSS3
ADAMDEC1
ADAMTS1
ADARB1
ADH1B
AGER
AKAP12
ANKRD29
ANXA3
AQP4
ARHGAP29
ARHGEF26
BMP5
C7
CACNA2D2
CAV1
CCDC141
CDHR3
CGNL1
CHRDL1
CLDN18
CLEC3B
CLIC5
COL10A1
COL1A1
COL3A1
CPB2
CTNNAL1
CXCL14
CYP4B1
DACH1
DOCK4
EDN1
EDNRB
EML1
EMP2
EPAS1
FABP4
FAM107A
FAM13C
FAM189A2
FAP

FBLN5
FCN3
FHL1
FHL5
FIGF
FILIP1
FOSB
GIMAP8
GJB2
GKN2
GLDN
GOLM1
GPR126
GPR133
GPX3
GREM1
GRK5
GUCY1A2
HBB
HHIP
HIGD1B
HMMR
HPGD
HSD17B6
IGSF10
IL1RL1
ITGA11
ITGA8
KIAA1324L
KLF4
LAMA3
LAMP3
LDB2
LEPREL1
LIFR
LIMCH1
LPHN2
LPL
LRRC36
LRRN3
LYVE1
MAMDC2
MMP1
MMP11
MMP12
MMP9
MYCT1
MYH10
NCALD

NCKAP5
NEBL
NEDD9
NOSTRIN
NPNT
NUSAP1
P2RY14
PALMD
PCOLCE2
PDE1C
PDK4
PDZD2
PEBP4
PGC
PHLDB2
PIP5K1B
PLA2G1B
PLAU
PLCB4
PLCE1
PLEKHH2
PPARGC1A
PREX2
PRG4
PTPN21
PTPRB
RTKN2
SASH1
SCEL
SCGB1A1
SCN7A
SDPR
SEMA6A
SFTPC
SFTPD
SLC39A8
SLC6A4
SLCO2A1
SOSTDC1
SPP1
SPTBN1
STEAP1
STXBP6
SULF1
SYNE1
TACC1
TCF21
TEK
TGFBR3

THBS2
TMEM100
TNNC1
TOP2A
TPX2
TSPAN12
TSPAN7
VEPH1
VIPR1
WIF1

Supplementary Table 3. The core targets of MHD against LC

Core targets
ABL1
ACTB
ADRB2
AKT1
AP2M1
APC
APP
AR
ARRB2
ATF2
AURKA
AURKB
BAG3
BAG6
BARD1
BMI1
BRCA1
BTRC
C1QBP
CALM1
CALM2
CALM3
CAND1
CANX
CAPZA2
CAV1
CBL
CCDC8
CDC37
CDC5L
CDK1
CDK2
CDKN1A
CEP250
CFL1

CFTR
CHD3
CHUK
CLTC
COMMD3-BMI1
COPS5
COPS6
CREBBP
CRK
CSNK2A1
CSNK2A2
CSNK2A3
CSNK2B
CTNNB1
CUL1
CUL2
CUL3
CUL4A
CUL4B
CUL5
CUL7
DAXX
DBN1
DCUN1D1
DDB1
DDX21
DHX15
DHX9
DYNC1H1
EED
EEF1A1
EEF2
EFTUD2
EGFR
EIF4A3
EMD
EP300
EPAS1
ESR1
EWSR1
EZH2
FAF2
FBXO6
FBXW11
FLNA
FN1
FUS
FYN
GRB2

GRK5
GSK3B
HDAC1
HDAC2
HDAC3
HDAC5
HDAC6
HIF1A
HIST1H3A
HIST1H3B
HIST1H3C
HIST1H3D
HIST1H3E
HIST1H3F
HIST1H3G
HIST1H3H
HIST1H3I
HIST1H3J
HNRNPA1
HNRNPL
HNRNPM
HNRNPU
HSP90AA1
HSP90AB1
HSPA4
HSPA5
HSPB1
HUWE1
IFI16
IKBKB
IKBKG
ILF3
IQGAP1
ITCH
ITGA4
JUN
JUP
KAT5
KDM1A
KHDRBS1
KPNB1
KRT18
LIMA1
LMNA
LRRK2
MAGOH
MAPK1
MAPK14
MAPK3

MAPRE1
MCM2
MCM5
MCM7
MED23
MED4
MYC
MYH10
MYH9
MYO1C
NCL
NCOR1
NEDD4
NEDD8
NFKB1
NFKBIA
NOP2
NOP56
NPM1
NR3C1
NTRK1
OBSL1
OTUB1
PAN2
PARP1
PAXIP1
PHB
PHB2
PIN1
PML
PPARG
PPARGC1A
PPP1CA
PPP1CB
PPP2CA
PPP2R1A
PRKDC
PSMD2
PSMD4
PTEN
RACK1
RAD21
RAF1
RANBP2
RB1
RBX1
RELA
RNF2
RPA1

RPA2
RPA3
RPL10
RPL13
RPL15
RPL3
RPL4
RPL5
RPS13
RUVBL1
RXRA
SFN
SFPQ
SH3KBP1
SHC1
SIN3A
SIRT1
SIRT7
SKP1
SMAD2
SMAD3
SMAD4
SMARCA4
SMARCC1
SMARCC2
SMURF1
SNCA
SNW1
SP1
SPTAN1
SPTBN1
SQSTM1
SRC
SRPK1
SRRM2
SRSF1
SRSF2
SSRP1
STAT1
STAU1
STUB1
SUZ12
TERF2
THRAP3
TMPO
TOP1
TOP2A
TP53
TRAF2

TRAF6
TUBA1A
TUBB
TUBG1
U2AF2
UBC
UBE2I
UBL4A
UCHL5
USP7
VCAM1
VCP
VHL
VIM
XPO1
XRCC5
YWHAB
YWHAE
YWHAG
YWHAQ
YWHAZ

A

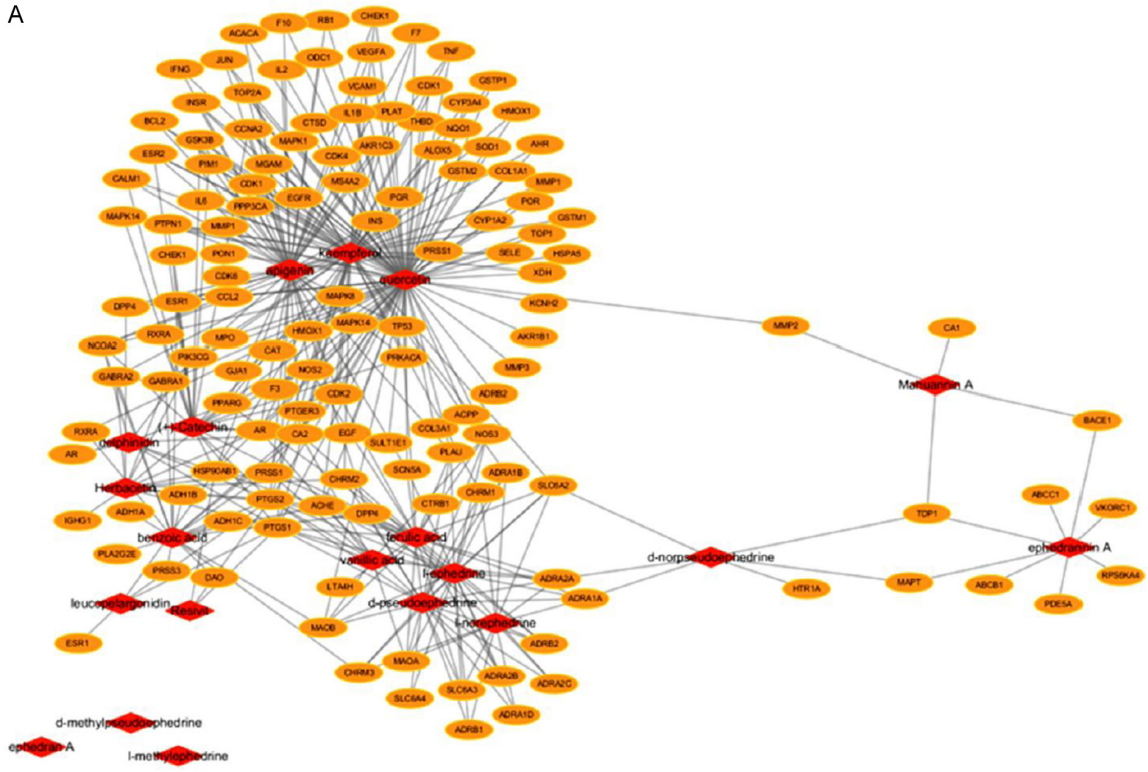

B

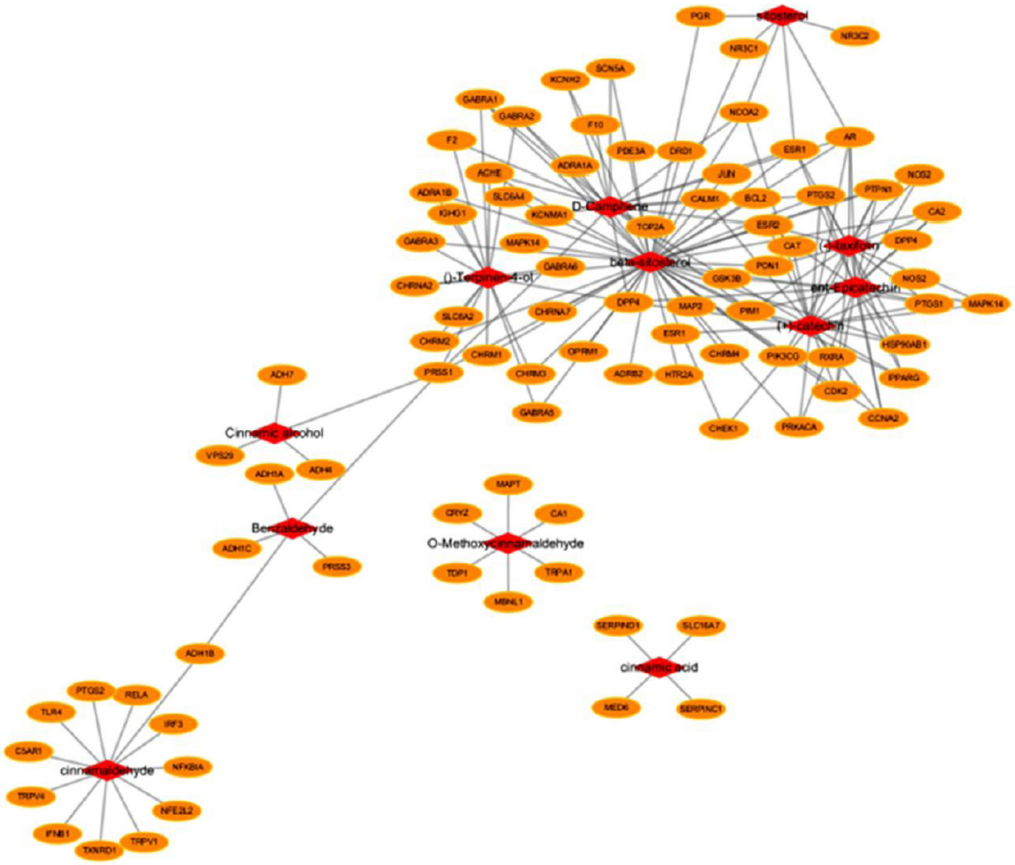
Cinnamic alcohol
Benzaldehyde
O-Methoxycinnamaldehyde
cinnamic acid
cinnamaldehyde
beta-sitosterol
D-Camphene
(+)-Catechin
ent-Epicatechin
(+)-taxifolin
D-Limonen-4-ol

C

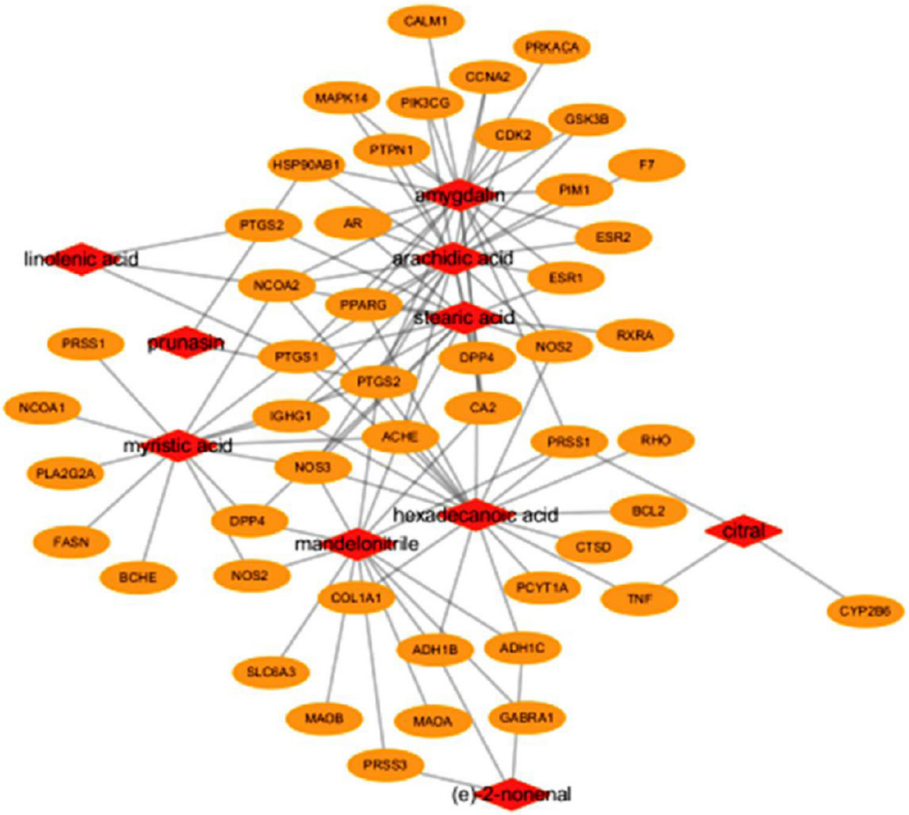
amygdalin
linolenic acid
arachidic acid
stearic acid
prunasin
myristic acid
hexadecanoic acid
mandelonitrile
citral
(e)-2-nonenal

D

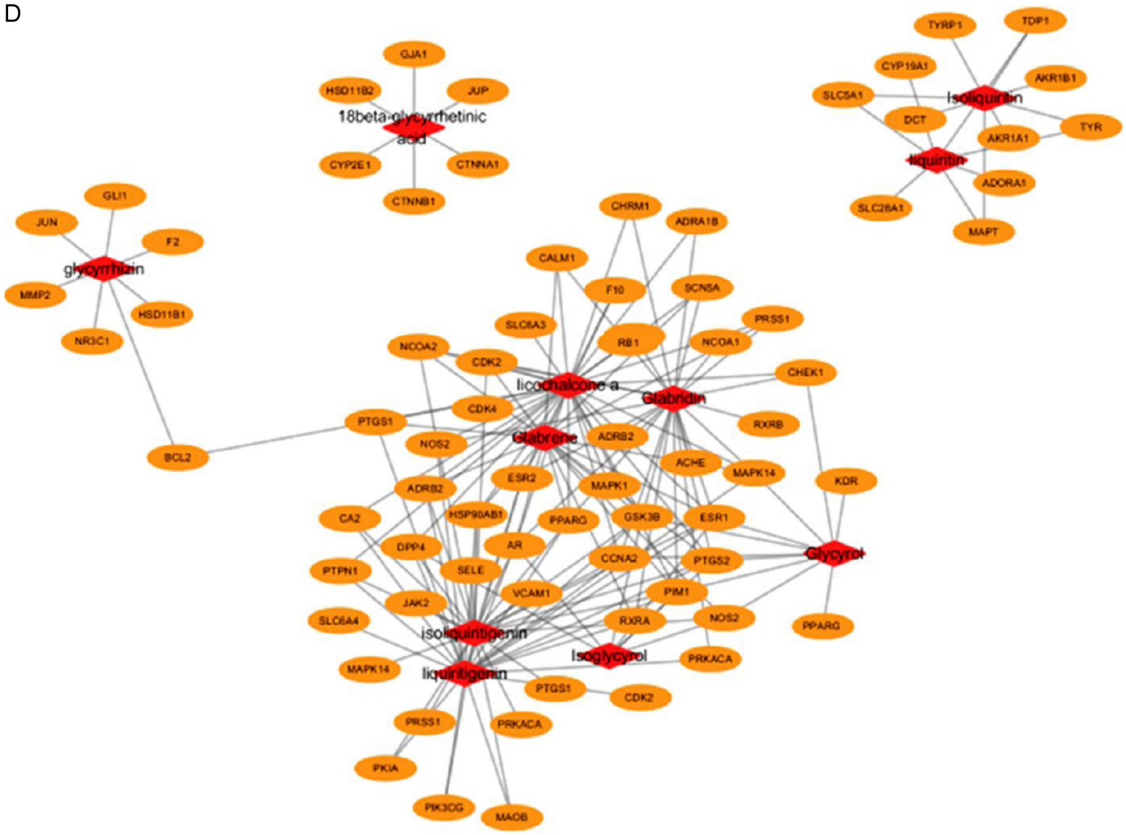

Supplementary Figure 1. Construction of the single herb related candidate active ingredient-putative target network. (A) Ephedrae Herba (Ma-Huang, MH) and its putative targets, (B) Cinnamomi Ramulus (Gui-Zhi, GZ) and its putative targets, (C) Armeniacae Semen Amarum (Xing-Ren, XR) and its putative targets, (D) Glycyrrhizae Radix Et Rhizoma (Gan-Cao, GC) and its putative targets.

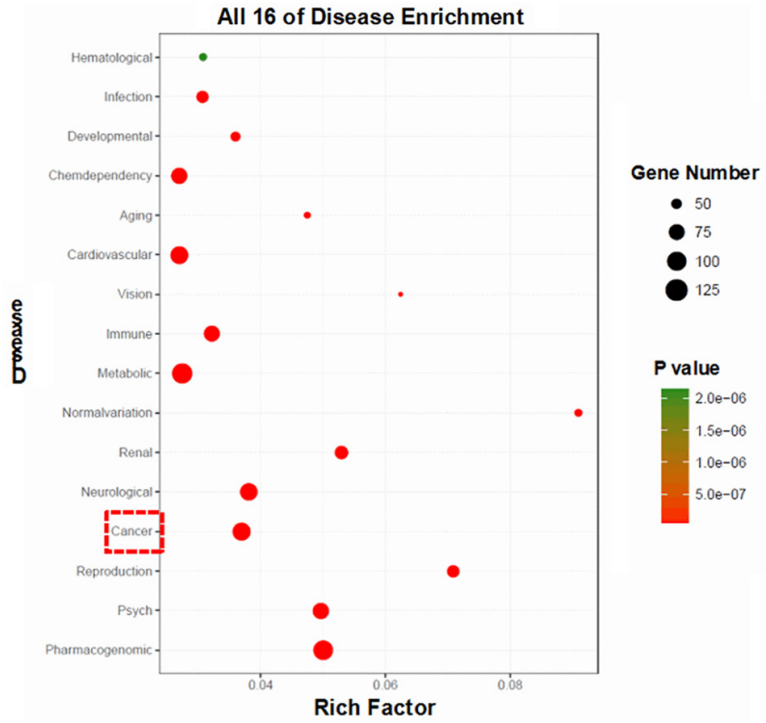

Supplementary Figure 2. Putative drug targets of MHD were enriched in the representative diseases using DAVID v6.8.

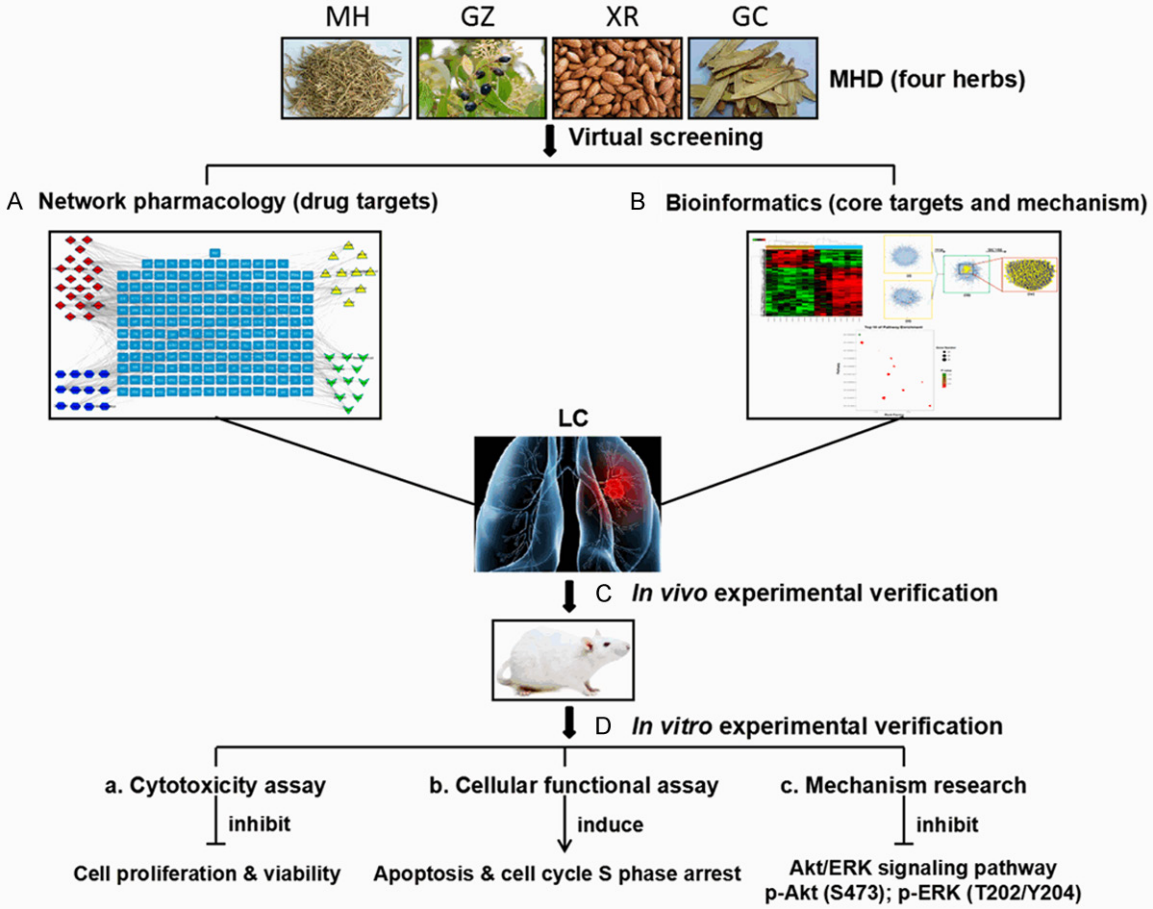

Supplementary Figure 3. The overall schematic design of this research. A. Starting the study with a network pharmacology technology and drug target prediction. B. An virtual study was conducted to explore the mechanism of MHD action on LC cells in the assistance of network pharmacology and bioinformatic analysis tools. C. Using *in vivo* assay to verify the inhibition effect of MHD on LC cells. D. The cytotoxicity test, cellular functional assay and mechanism research to assess and verify the above predicted biological functional and signaling pathways related to MHD on LC cells using by serial *in vitro* assays.

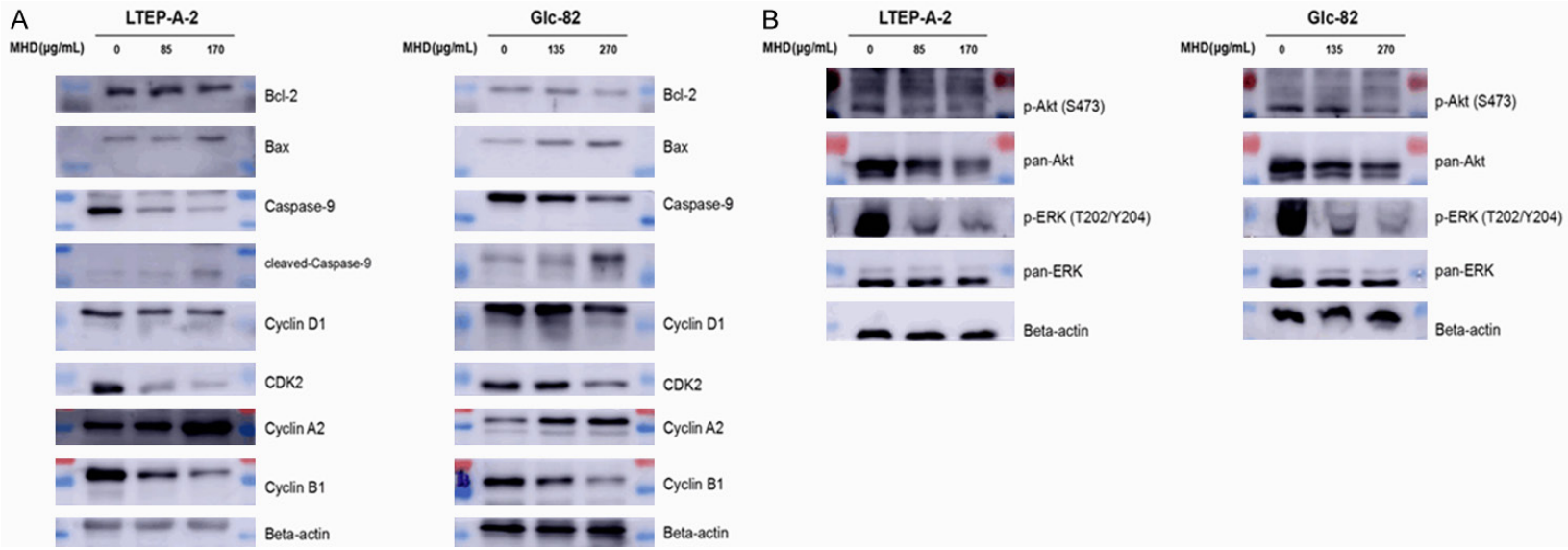

Supplementary Figure 4. The original western blot images.